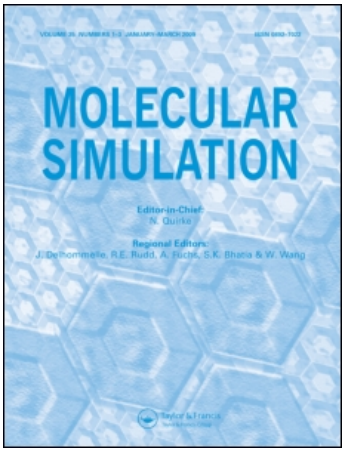

Molecular Simulation
Publication details, including instructions for authors and subscription information:
http://www.informaworld.com/smpp/title~content=t713644482

Theoretical Analysis of Computer Simulations of Sorption in a Cylindrical Micropore

M. J. Bojan[a]; W. A. Steele[a]
[a] Department of Chemistry, The Pennsylvania State University, University Park, PA

To cite this Article Bojan, M. J. and Steele, W. A.(1996) 'Theoretical Analysis of Computer Simulations of Sorption in a Cylindrical Micropore', Molecular Simulation, 17: 4, 303 — 315
To link to this Article: DOI: 10.1080/08927029608024114
URL: http://dx.doi.org/10.1080/08927029608024114

Molecular Simulation, 1996, Vol. 17, pp. 303–315
Reprints available directly from the publisher
Photocopying permitted by license only

THEORETICAL ANALYSIS OF COMPUTER SIMULATIONS OF SORPTION IN A CYLINDRICAL MICROPORE

M. J. BOJAN and W. A. STEELE

Department of Chemistry The Pennsylvania State University
University Park, PA 16802

(Received January 1996; accepted February 1996)

The simulation of krypton in a cylindrical pore with atomically rough walls is reconsidered. Distributions of gas-gas, gas-solid and total energy are presented and discussed in terms of their ability to characterize the adsorbed phase, especially by assigning sorbed atoms to layers within the pore. The calculation of the chemical potential of the sorbed phase from the distributions of the total energy per particle is presented and an approximate method of splitting the chemical potential into contributions due to the gas-gas and gas-solid energies is suggested and tested against the simulation data. It is found that the approximation works reasonably well for coverages up to monolayer, but shows significant deviations from the simulated values at coverages corresponding to the nearly full pore.

Keywords: Cylindrical micropore; krypton; rough walls

1. INTRODUCTION

The use of computer simulations to evaluate the thermodynamic and dynamical properties of model physically adsorbed films is a powerful method of validating models by comparison of their simulated properties with those of real systems. In addition, one can extract considerable information from a carefully planned simulation that is not available from macroscopic measurements. An obvious example is the simulation of local microscopic densities that tell one the most probable positions of the molecules relative to the adsorbent surface or, in a porous solid, where they are relative to the pore walls [1]. Such information is particularly revealing when the adsorbent is heterogeneous, which means that some portions of the surface have stronger interactions with an adsorbed gas than others.

Furthermore, the dependence of these distributions upon the amount of adsorbed material can be an extremely helpful diagnostic tool, especially in the neighborhood of a phase transition in the adsorbed layer (or in the fluid sorbed in a pore). Such distributions can be extracted from either Monte Carlo or molecular dynamics simulations, since each is capable of generating the molecular configurations that are characteristic of the statistical ensembles that represent the adsorption system [2, 3]. These would be constant T, V and chemical potential μ for a Grand Canonical Monte Carlo (GCMC) simulation, and constant T, N, V for the most popular molecular dynamics algorithm. In addition to giving a valuable visual picture of the details of the adsorption process, density distributions enable one to evaluate averages of various functions of N, the number of adsorbed molecules. (Of course, these calculations are only of interest in GCMC and other simulations in which N is a fluctuating variable rather than a fixed quantity.) For example, evaluation of $\langle N \rangle$or of $\langle N^2 \rangle$ can be done by integrating over the histogram of the local density of molecules times the density or the density squared. (In the Grand Canonical ensemble, the derivative of the chemical potential with respect to N is proportional to the fluctuation in N, which ultimately allows one to calculate the slope of the adsorption isotherm.) Other histograms can be constructed, and the ones that will be of interest in the present paper are those involving the potential energy of the particles in the adsorbed fluid.

In most models of the physical adsorption process [4], two assumptions are made at the outset: that the interactions between adsorbed molecules can be written as a sum over all pairs, and that the interaction of a molecule with the solid adsorbent can be written as a sum over sites in the solid. (This implies that the solid remains unaffected by the adsorption process and plays the role of an external field of force acting upon each particle in its vicinity.) We define $u_{gg}(\mathbf{r}_{ij})$ as the interaction between a pair of sorbate atoms i and j separated by $\mathbf{r}_{ij}$. Also, the interaction of atom i with the solid adsorbent will be denoted by $\varepsilon_{gs}(\mathbf{r}_i)$, where $\mathbf{r}_i$ is the position of the molecule relative to the solid. Evidently, this model gives the potential energy of an atom at $\mathbf{r}_i$ that is due to its interactions with its neighbors in the sorbed film as half the sum of $u_{gg}(\mathbf{r}_{ij})$ over all other atoms j (with $j \neq i$); we denote this by $\varepsilon_{gg}(\mathbf{r}_i)$. (We assign half the energy of an interacting pair to each molecule in the pair.) Finally, the total potential energy of this molecule is denoted by $\varepsilon_{tot}(\mathbf{r}_i)$; it is just the sum of the two component parts defined here.

Here, we will discuss some properties of the distributions of these energies. In particular, we will evaluate $f(e_{gs})de_{gs}$, the number of sorbed mol-

ecules in the system with gas-solid energies between e_{gs} and $e_{gs} + de_{gs}$, and the analogous functions for e_{gg} and e_{tot}. Here, we use the energy e rather than ε because the position variable $\mathbf{r}$ is no longer relevant or, to put it more precisely, because one averages over all $\mathbf{r}$ in the system in order to get the number of molecules having a given energy regardless of their position. In effect, the simulation algorithm generates a lengthy sequence of molecular configurations which correspond to those in the chosen ensemble. One evaluates the potential energies of each molecule in each configuration and assigns it to a bin with energy between e_x and $e_x + \delta e_x$, where $x =$ gg, gs, or tot. Division by the number of configurations scanned then gives the histogram or, in the limit of small bin width, $f(e_x)$ the distribution of the energy times de_x.

The normalization of these functions is chosen here such that

$$N = \int f(e_x) de_x \tag{1}$$

where N is the number of adsorbed particles in the system. The averages of the n'th powers of the energies of these atoms are also trivially given by:

$$\langle (u_x)^n \rangle = \frac{1}{N} \int (e_x)^n f(e_x) de_x \tag{2}$$

Of course, these averages can be more easily calculated directly during the simulations. In previous studies, these distributions were used as a tool for visualizing where the energies of the adsorbed atom come from and how they change with coverage N. This paper will be primarily concerned with the relationship between the energy distributions and the chemical potential of the adsorbed phase.

This argument starts from the well-known (rigorous) equation [5] which states that

$$e^{(\mu - \mu_{id})/\mathrm{kT}} = \langle e^{e_{tot}/\mathrm{kT}} \rangle \tag{3}$$

where μ_{id} is the chemical potential of the ideal gas with the same number of molecules, V, T as the adsorbed fluid with chemical potential μ. Thus,

$$\frac{\mu_{id}}{\mathrm{kT}} = \ln \frac{N\Lambda^3}{V} \tag{4}$$

with $\Lambda = h/(2\pi mkT)^{1/2}$ for atoms. Also,

$$\langle e^{e_{tot}/kT} \rangle = \int e^{e_{tot}/kT} f(e_{tot}) de_{tot} \tag{5}$$

For bulk fluids, eqs. 3 and 5 give only one of a number of methods that have been employed to evaluate chemical potentials. In fact, it has been shown that this method is not as accurate as several of the alternatives [6], so it is not very popular at present. One question that we wish to explore here is whether one can split the chemical potential of the adsorbed film into the sum of two terms, one associated with the effect of the gas-solid interactions upon the chemical potential of the adsorbed fluid, which will be denoted by μ_{gs}, and a second term associated with the contribution of the gas-gas interactions to the overall chemical potential, which will be denoted by μ_{gg}. Perhaps the best known approximate theory of this kind is the Frenkel-Halsey-Hill (F.H.H.) theory [4], in which one writes the chemical potential and thus the adsorption isotherm of the thick film as the sum of the bulk fluid chemical potential which depends only upon the gas-gas interactions and a term that takes account of the effect of the gas-solid energy upon the chemical potential. Here, we will examine the validity of the assumption that the chemical potential can be written as the sum of gas-solid and gas-gas contributions.

In the next section, we describe a simulation that will be used as a basis for this study. Subsequently, we present the theoretical ideas that we wish to examine, and compare the predictions of the theory with the simulated properties for the system considered. Finally, a brief discussion of the meaning of these calculations and the prospects for their extensions to other types of adsorption systems are presented.

2. COMPUTER SIMULATIONS

Grand Canonical Monte Carlo simulations were performed for krypton in a straight-walled cylindrical pore at 120 K [7]. The algorithm used is conventional for sorption in a pore [3,8]. The isotherm and the atomic configurations were obtained by increasing the pressure of the gas in equilibrium with the sorbed phase in small increments and simulating the system at each point. In the simulation for a given pressure, displacement, creation and destruction trials occurred with equal frequency. Equilibrium was reached after 10^6 trials, and data was gathered for 5.10^5 trials. To check

the precision of the results, runs six times longer were carried out for three pressure values. No significant difference was observed between these and the corresponding standard length run.

The krypton is a Lennard-Jones gas with pair-wise inverse 12–6 power law interactions. The well depth and size parameter taken are standard for this gas: $\varepsilon/k = 170$ K and $\sigma = 3.60$ Å. The Kr-pore wall interactions were assumed to be a pair-wise sum over atomic sites in the solid adsorbent. The parameters for the site-Kr 12–6 interactions were taken to be $\varepsilon/k = 101$ K and $\sigma = 3.45$ Å [7]. The site positions were those for an amorphous material - specifically, those for a randomly-packed array of spheres. This model has been discussed in detail elsewhere [9]. Here, we note that the wall of the pore studied is rough on an atomic scale and thus presents an energetically heterogeneous adsorbing surface. The pore has a length of 41 Å in the direction of the periodic boundary condition and a nominal diameter of 10 Å. (This is actually the observed value of the average radius of the outermost cylinder of adsorbed atoms–see Fig. 3). The volume and area available to the Kr in this pore are $\simeq$ 14000 Å^3 and 2600 Å^2. In the previous study, it was shown that capillary condensation occurs in this pore together with a hysteresis loop having vertical branches. Here, we focus on the properties at pore fillings above and below this condensation regime, with only a few results shown for pore fillings on the condensation branch. (For GCMC simulations, coverage jumps discontinously when condensation occurs; in order to gain any information at all for pore fillings in the vertical regime of the isotherm, one must resort to Canonical ensemble simulations.)

As shown elsewhere [7], the simulations give the monolayer coverage of Kr in this pore as 160 atoms and a pore-filling value of 330 atoms, with uncertainties of less than 5%. (Thus, the area per Kr in the monolayer is estimated to be 16.3 Å^2.) The vertical condensation step in the adsorption isotherm extends from $\simeq$ 170 atoms to $\simeq$ 300 atoms.

Figures 1 and 2 show distributions of the gas-gas and gas-solid energies of krypton in this model pore for a variety of pore fillings ranging from a fraction of a monolayer up to an essentially full pore. The variation in the local density $\rho(R)$ with distance R from the pore axis that is shown in Figure 3 indicates that the sorbed phase in a nearly full pore has considerable structure consisting of well-defined first, second and third layers (that are cylindrical shells of atoms) and a poorly defined fourth "layer" near the pore axis. For this (and other) pore filling values, an appropriate integral under a peak in the density plot gives the number of atoms in each of these layers; alternatively, the integral under the first layer peak in a gas-solid

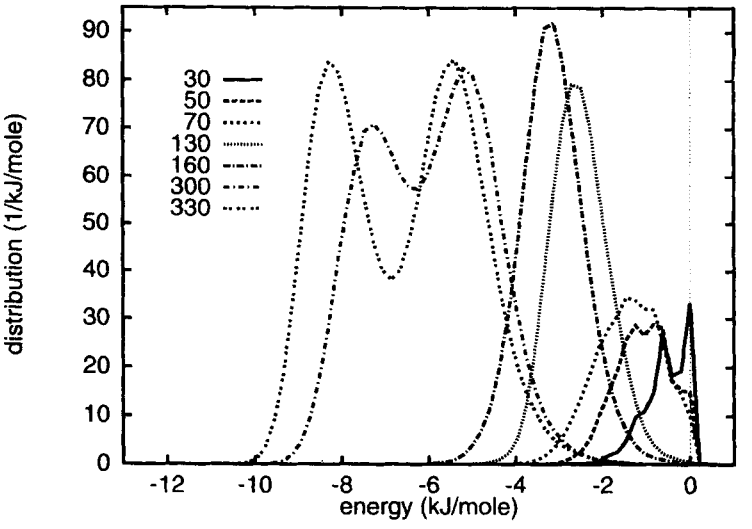

FIGURE 1 Distributions of the Kr-Kr pair interaction energy are plotted versus e_{Kr-Kr} for a number of pore filling values. Curves for N less than 160 are submonolayer; those for $N = 300$ and 330 correspond to the nearly full pore.

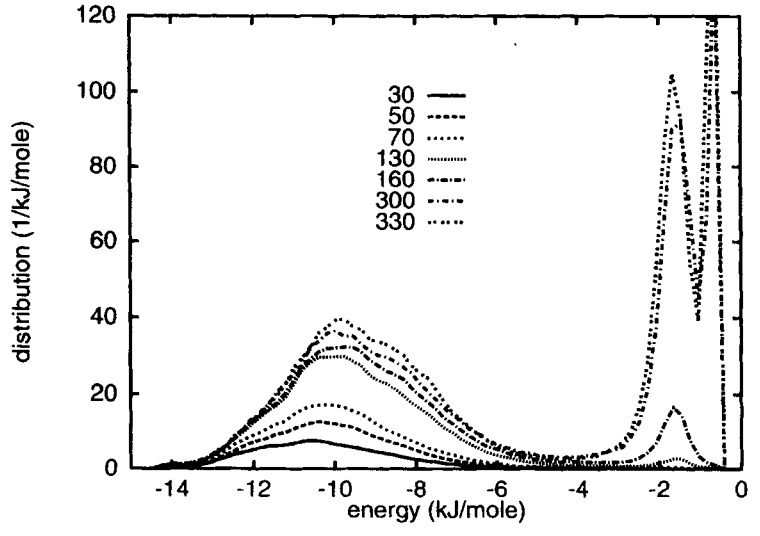

FIGURE 2 Same as Figure 1, except that the energy in this case is the gas-solid e_{Kr-s}.

energy distribution of Figure 2 for $N = 300$ or 330 also gives the occupancy in the first layer. (These two methods of calculation are consistent with one another and give the monolayer number cited above.)

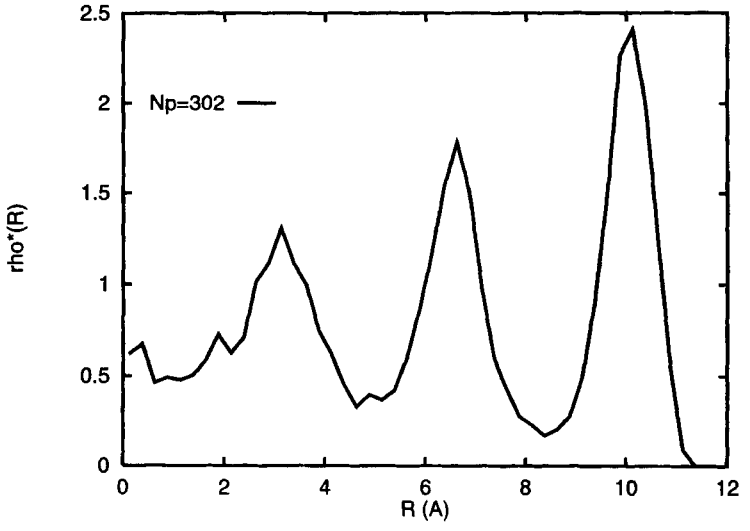

FIGURE 3 Local density (in reduced units) is plotted as a function of distance R from the pore axis. The curve shown is for a nearly full pore with $N = 302$. The reduced density is defined as $\rho^* = \rho \times \sigma_{gs}^3$, where ρ is in units of atoms/Å^3.

The gas-solid energy distributions in Figure 2 clearly show broad peaks ranging from $\simeq -14$ kJ/mole to $\simeq -4$ kJ/mole. These are due to interactions of atoms in the first sorbed layer with the adjacent heterogeneous pore wall. Because of the normalization chosen for these curves, the peak heights for submonolayer coverages increase almost proportionally to the amount adsorbed. Note that these peaks show that sorption does not occur only on the strong energy sites at low coverage, followed by sorption on the areas of weaker interaction at higher coverages, as is often assumed in descriptions of adsorption on a heterogeneous surface [10, 11]. In fact, the changes in the shapes of these peaks that occur as coverage increases are gradual, and surprisingly, continue even at much higher coverages of 300 and 330 atoms where one might have thought that the first layer was complete and merely serving as an inert surface for the atoms adsorbed in the higher layers. The beginning of sorption in the second layer is clearly seen by the appearance (at $N = 130$) of a peak at $\simeq -1.5$ kJ/mole. Sorption in the interior of the pore is the source of the sharp peak that appears at $\simeq -0.5$ kJ/mole for the two highest values of the pore filling. Average gas-solid energies calculated from these distributions agree well with the directly simulated values. They show a linear increase from -10.7 kJ/mole in the limit of zero coverage to -9.0 kJ/mole at 150 atoms; at higher pore filling values than 150, the rate

of increase steepens as sorption in the second layer and interior volume of the pore increases.

At the lowest coverage of 30 atoms (0.2 monolayer), the distribution of Kr-Kr energies shown in Figure 1 indicates that some of the atoms are isolated (the peak at $\simeq 0$ kJ/mole), most of the atoms present as pairs (with an energy of $\simeq$ 0.7 kJ/mole per atom in the pair) or as triplet clusters. The curves for 130 and 160 atoms show how the interaction energy is distributed in a two-dimensional fluid. The Kr-Kr distributions at the two highest coverages are split into two peaks, one for those atoms that are near the surface and thus are missing some of the nearest neighbors that would be present in the three-dimensional fluid, and a second peak for the fluid in the pore interior. The second peak in the distributions for the sorbed fluid is close to that for the bulk, which has a single peak with a maximum at $-$ 8.5 kJ/mole, only for the completely filled pore.

3. CHEMICAL POTENTIAL

The primary goal of this paper is to discuss the question of whether the chemical potential of the adsorbed phase can be split into a gas-gas plus a gas-solid term. From eqns. 3 and 5, we have

$$\frac{\mu_{tot}}{kT} - \frac{\mu_{id}}{kT} = \ln \int e^{e_{tot}/kT} f(e_{tot}) de_{tot} = \ln \langle e^{(e_{gs} + e_{gg})/kT} \rangle \tag{6}$$

We would like to write

$$\ln \langle e^{(e_{gs} + e_{gg})/kT} \rangle = \frac{\mu_{gs}}{kT} + \frac{\mu_{gg}}{kT} \tag{7}$$

with

$$\frac{\mu_{gs}}{kT} = \ln \int e^{e_{gs}/kT} f(e_{gs}) de_{gs} \tag{8}$$

and

$$\frac{\mu_{gg}}{kT} = \ln \int e^{e_{gg}/kT} f(e_{gg}) de_{gg} \tag{9}$$

It is evident that several approximations have been made in writing eq. 7. Their numerical accuracy will be explored to some extent below, but here we note that perhaps the most significant approximation that is being made here is that $f(e_{gg})$ and $f(e_{gs})$ are independent functions, when in fact they both depend completely upon the configurations of the atoms in the pore for a given statistical ensemble. In fact, if these two distributions are independent of one another, there is a convolution relation that gives $f(e_{tot})$ in terms of the two component parts:

$$f(e_{tot}) = \frac{1}{N_p}\int f(e_{gg})f(e_{gs})\delta(e_{gs} + e_{gg} - e_{tot})de_{gs}de_{gg} \tag{10}$$

After integrating over e_{gs}, one has

$$f(e_{tot}) = \frac{1}{N_p}\int f(e_{gg})f(e_{tot} - e_{gg})de_{gg} \tag{11}$$

where the second function in the integral is actually the distribution for the gas-solid energy, evaluated at $e_{gs} = e_{tot} - e_{gg}$.

The predictions of this convolution equation are compared with the directly simulated curves of $f(e_{tot})$ obtained in this study for a number of pore filling values in Figures 4–6. It is evident that the comparison is moderately good at submonolayer coverages, and deteriorates as the number of atoms in the pore approaches the maximum of 330.

With this agreement indicating that the coupling between the gs and the gg distribution functions is not so large, we are in a position to test the idea that this theory is capable of reproducing the N-dependence of chemical potential obtained in the GCMC simulation. For Kr at 120 K, $\Lambda^3 = 5.3 \cdot 10^{-3}\text{Å}^3$ so that eq. 4 gives

$$\frac{\mu_{tot} - \mu_{id}}{kT} = \frac{\mu_{sim}}{RT} - 14.8 + \ln N \tag{12}$$

In the previous work, the isotherm, expressed as μ_{sim}/RT as a function of the average N, was evaluated in the GCMC simulation [7]. These data are used in Figure 7 to plot the krypton isotherm according to the right-hand-side of eq. 12. Also shown in Figure 7 are $\mu_{gs}/kT, \mu_{gg}/kT$, their sum, and the average of $(\mu_{tot} - \mu_{id})/kT$ evaluated from eq. 6 and the simulated $f(e_{tot})$.

Note first that eq. 7 approaches Henry's Law constant in the limit of small $\langle N \rangle$. In this case, μ_{gg}/kT must approach zero ($e_{gg} = 0$ when there are

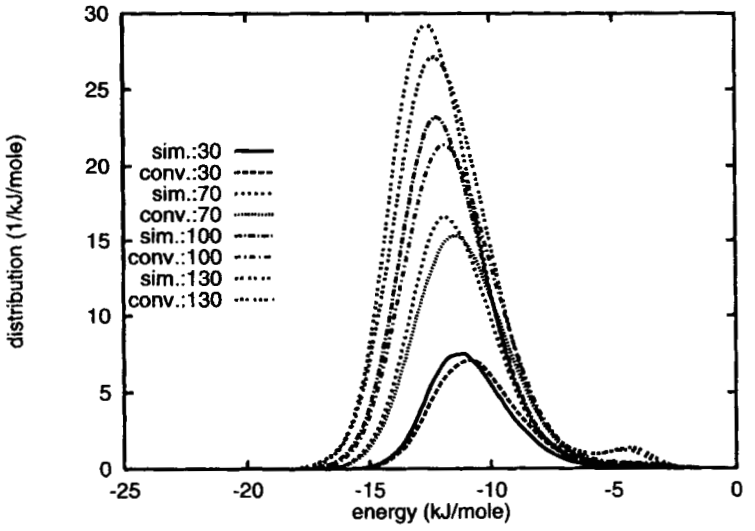

FIGURE 4 Tests of the convolution approximation for the calculation of the distribution of the total energy e_{tot} are shown here. "sim" denotes the directly simulated distributions, and "conv" denotes the distribution calculated from eq. 11. All curves shown are for submonolayer coverages.

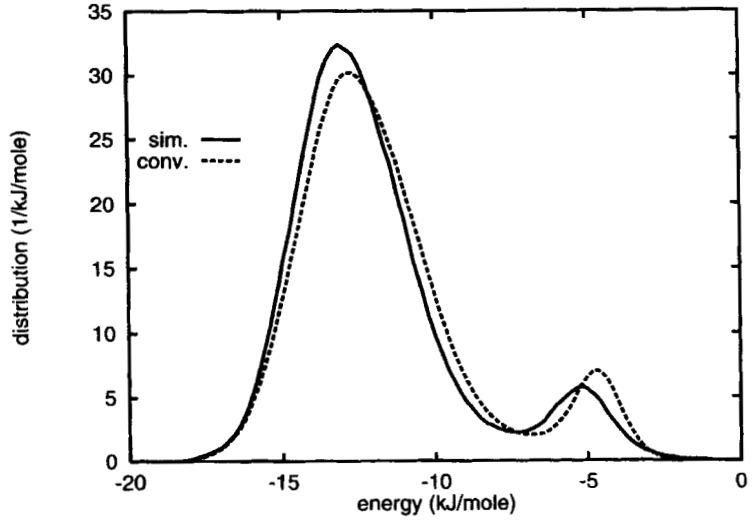

FIGURE 5 Same as Figure 4, but for the nominal monolayer coverage; the small peak at $\simeq -5$ kJ/mole is due to the presence of some second layer atoms at 120 K for $N = 160$.

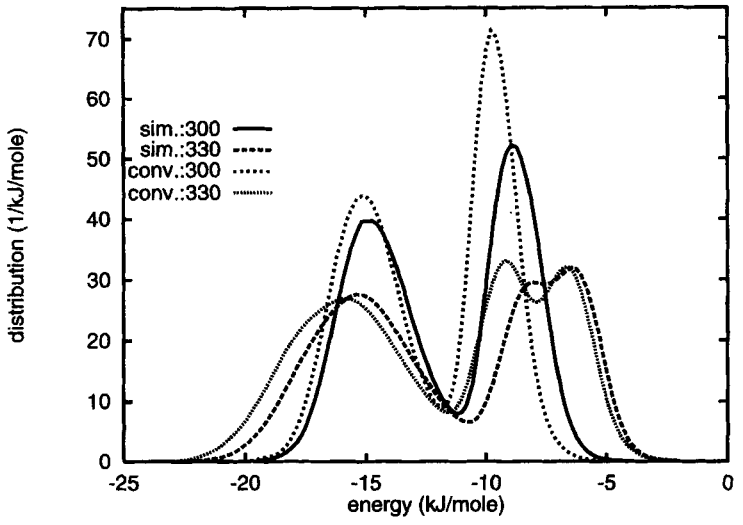

FIGURE 6 Same as Figure 4, but for two values of N corresponding to the nearly filled pore.

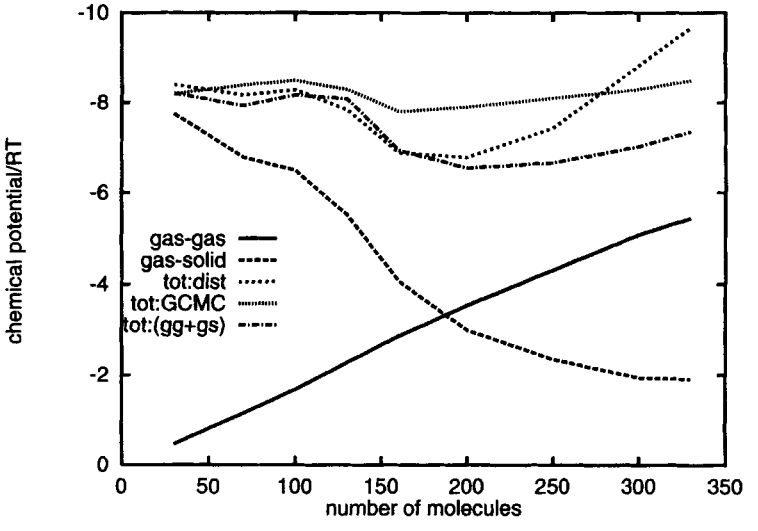

FIGURE 7 The various chemical potentials evaluated here are shown as a function of N, the number of atoms in the pore. Detailed descriptions of these chemical potentials are given in Sec. 3.

no Kr neighbors to an adsorbed atom). However, the present estimation of Henry's Law constant is quite different than the usual one, which is based on an integral over $\mathbf{r}$ of $e^{(-e_{gs}(\mathbf{r})/kT)}$. In the present case, we are setting the

Henry's Law constant equal to the reciprocal of the integral of the low coverage limiting form of $f(e_{gs})$ over e_{gs}. If the constant is defined by $N = pK_H$ in the limiting regime, then

$$\frac{\mu_{tot} - \mu_{id}}{kT} = \ln \frac{V}{K_H kT} \tag{13}$$

A conventional evaluation of K_H gives $2.18 \cdot 10^3$ molecules/atm. so the right-hand-side of eq. 13 is -7.6, in moderate agreement with the alternative value which equals -8.2 ± 0.2 as can be seen in Figure 7.

At finite coverages, there are several features of note in Figure 7: First, the sum of μ_{gg}/kT and μ_{gs}/kT is quite close to the directly calculated μ_{tot}/kT for coverages up to the point of condensation ($N = 160$). Second, these curves agree rather well with the GCMC simulation of μ_{tot} up to roughly monolayer coverage; above this, the divergence is most likely due to the same kind of problem in accurately evaluating the integrals encountered in the calculations for bulk fluids [6]; there is a large contribution to the integrand from energies that are large and positive and since there are only a few molecules with such energies, it is difficult to evaluate the distribution functions in this regime with sufficient accuracy to give a satisfactory value for the integral; Third, μ_{gs} continues to change for total coverages where the adsorption is occurring primarily in the pore interior; it seems likely that the atoms in the interior are perturbing those in the first layer where μ_{gs}/kT is large and negative. (This can be seen in the curves of $f(e_{gs})$ shown in Fig. 2). Fourth, μ_{gg}/kT varies almost linearly with N over the entire range of coverage. As unlikely as this is, it suggests that an expansion of this chemical potential in powers of N could be truncated at the linear term, and that a calculation of this "second virial" coefficient might be of interest; note that one expects that μ_{gg}/kT will approach the value for the bulk liquid which is equal to -6.1 at 120 K. Finally, there is nothing in these curves that corresponds to the model of the F.H.H. theory. Why this is so for such a well-regarded description of multilayer adsorption is an open question which can be best answered by extending the calculations of this paper to isotherms simulated for flat surfaces.

Acknowledgement

Support for this research was provided by grant DMR 9022681 of the N.S.F. Division of Material Research.

References

[1] Bojan, M. J. and Steele, W. A. (1994) "Simulations of Sorption in Pores with Constrictions", in *Characterization of Porous Solids* III, ed. Rouquerol, J., Rodriguez-Reinoso, F. and Sing, K. S. W. Unger, K. K. (Elsevier, Amsterdam), p. 11 – 20.
[2] Haile, J. M. (1992) "*Molecular Dynamics Simulation*" (John Wiley and Sons), New York.
[3] Allen, M. P. and Tildesley, D. J. (1987) "*Computer Simulation of Liquids*" (Oxford University Press, Oxford).
[4] Steele W. A. (1974) "*The Interaction of Gases with Solid Surfaces*, (Pergamon Press, Oxford), chap. 5.
[5] Rowlinson, J. S. and Widom, B. (1982) "*Molecular Theory of Capillarity*" (Oxford University Press, Oxford), sec. 4.2.
[6] Powles, J. G. (1982) "The computation of the chemical potential of a fluid", *Chem. Phys. Lett.*, **86**, 335–339; Powles, J. G., Evans, W. A. B. and Quirke, N. "Non-destructive molecular dynamics simulation of the chemical potential of a fluid", *Molec. Phys.*, **46**, 1347 – 1370; Guillot, B. and Guissani, Y., " Investigation of the chemical potential by molecular dynamics simulation", *Molec. Phys.*, **54**, 455 – 465.
[7] Bojan, M. J. and Steele, W. A. (1995) "Computer Simulations of Sorption in Model Cylindrical Pores", Proceedings, 5th Conference on *Fundamentals of Adsorption*, Asilomar, ed. D. LeVan (Kluwer, Amsterdam, 1996).
[8] Cracknell, R. F., Gubbins, K. E., Maddox, M. and Nicholson, D. (1995) "Modeling Fluid Behavior in Well-Characterized Porous Materials", *Acc. Chem. Res.*, **28**, 281 – 288.
[9] Bakaev, V. A. (1988) "Towards the Molecular Theory of Physical Adsorption on Heterogeneous Surfaces", *Surf. Sci.*, **198**, 571 – 592; Bakaev, V. A. and Steele, W. A. (1992) "Computer Simulation of the Adsorption of Argon on the Surface of Titanium Dioxide. 2. Amorphous Surface", *Langmuir* **8**, 1379–1384; Bakaev, V. A. and Steele, W. A. (1996) "Computer Simulation of Adsorption on Amorphous Oxide Surfaces", in *Adsorption and Chemisorption on Inorganic Sorbents.* (Studies in Surface Science and Catalysis, **99**) ed. Dabrowski, A. and Tertykh, V. A., (Elsevier, Amsterdam).
[10] Rudzinski, W. and Everett, D. H. (1992) "Adsorption of Gases on Heterogeneous Surfaces" (*Academic*, London).
[11] Jaroniec, M. and Madey, R. (1988) *Physical Adsorption on Heterogeneous Surfaces*, (Elsevier, Amsterdam).